Head-to-Head Comparison of T1 Mapping and Electroanatomical Voltage Mapping in Patients With Ventricular Arrhythmias

Sramko, Marek; Abdel-Kafi, Saif; Wijnmaalen, Adrianus P.; Tao, Qian; van der Geest, Rob J.; Lamb, Hildo J.; Zeppenfeld, Katja

Important note
To cite this publication, please use the final published version (if applicable).
Please check the document version above.

ORIGINAL RESEARCH

Head-to-Head Comparison of T1 Mapping and Electroanatomical Voltage Mapping in Patients With Ventricular Arrhythmias

Marek Sramko, MD, PhD,[a,b,*] Saif Abdel-Kafi, MD,[c,d,*] Adrianus P. Wijnmaalen, MD, PhD,[c,d] Qian Tao, PhD,[e]
Rob J. van der Geest, PhD,[f] Hildo J. Lamb, MD, PhD,[g] Katja Zeppenfeld, MD, PhD[c,d]

ABSTRACT

BACKGROUND Electroanatomical voltage mapping (EAVM) has been compared with late gadolinium enhancement cardiovascular magnetic resonance (LGE-CMR), which cannot delineate diffuse fibrosis. T1-mapping CMR overcomes the limitations of LGE-CMR, but it has not been directly compared against EAVM.

OBJECTIVES This study aims to assess the relationship between left ventricular (LV) endocardial voltage obtained by EAVM and extracellular volume (ECV) obtained by T1 mapping.

METHODS The study investigated patients who underwent endocardial EAVM for ventricular arrhythmias (CARTO 3, Biosense Webster) together with preprocedural contrast-enhanced T1 mapping (Ingenia 3T, Philips Healthcare). After image integration, EAVM datapoints were projected onto LGE-CMR and ECV-encoded images. Average values of unipolar voltage (UV), bipolar voltage (BV), LGE transmurality, and ECV were merged from corresponding cardiac segments (6 per slice) and pooled for analysis.

RESULTS The analysis included data from 628 segments from 18 patients (57 ± 13 years of age, 17% females, LV ejection fraction 48% ± 14%, nonischemic/ischemic cardiomyopathy/controls: 8/6/4 patients). Based on the 95th and 5th percentile values obtained from the controls, ECV >33%, BV <2.9 mV, and UV <6.7 mV were considered abnormal. There was a significant inverse association between voltage and ECV, but only in segments with abnormal ECV. Increased ECV could predict abnormal BV and UV with acceptable accuracy (area under the curve of 0.78 [95% CI: 0.74-0.83] and 0.84 [95% CI: 0.79-0.88]).

CONCLUSIONS This study found a significant inverse relationship between LV endocardial voltage and ECV. Real-time integration of T1 mapping may guide catheter mapping and may allow identification of areas of diffuse fibrosis potentially related to ventricular arrhythmias. (J Am Coll Cardiol EP 2023;9:740-748) © 2023 Published by Elsevier on behalf of the American College of Cardiology Foundation.

Currently, identification of fibrotic substrate of ventricular arrhythmias in patients with ischemic heart disease (IHD) and nonischemic cardiomyopathies (NICMs) relies on electroanatomical voltage mapping (EAVM). A region of interest with increased fibrosis can be approximated by a finding of abnormally decreased unipolar voltage (UV) and bipolar voltage (BV). Various voltage cutoffs have been suggested.[1] For clinical use, the voltage cutoffs require direct validation by histology or, alternatively, by cardiac magnetic resonance (CMR) imaging.[2-6]

Earlier studies have validated voltage cutoffs for fibrosis against conventional late gadolinium enhancement (LGE) CMR.[4] However, quantification of fibrosis by LGE-CMR also relies on various and inconsistent signal intensity thresholds, and it cannot reliably detect diffuse fibrosis, which occurs in NICM or in remote myocardium in patients with postinfarct left ventricular (LV) remodeling. Limitations of LGE-CMR to detect diffuse fibrosis can be overcome by the CMR technique of T1 mapping, which has been validated against histology.[7,8]

Previous studies have correlated native T1 values with occurrence of ventricular arrhythmias, pre- and postcontrast T1 values with all-cause mortality, and postcontrast T1 values with EAVM.[8-11] T1 mapping was restricted to a small region of interest in the interventricular septum, unfoundedly assuming uniform distribution of fibrosis throughout the LV myocardium. A direct comparison of EAVM and T1 mapping of the entire LV myocardium has not yet been performed.

The purpose of the study was to assess the relationship between LV endocardial voltage obtained by EAVM and extracellular volume (ECV) obtained by T1 mapping. To this end, we used 3-dimensional (3D) integration and reversed registration of EAVM with whole-heart precontrast/postcontrast T1 mapping in patients with ventricular arrhythmias and in control patients without structural heart disease (SHD).

METHODS

STUDY POPULATION. The study population consisted of consecutive patients who underwent endocardial EAVM for diagnosis and treatment of ventricular arrhythmias together with preprocedural CMR with contrast-enhanced T1 mapping and LGE. To ensure image quality, patients with implanted devices were excluded. Approval of the study by the institutional ethics committee was not required as all the performed procedures were part of a routine clinical protocol. All patients provided informed consent to the procedures.

CMR IMAGING. CMR was performed on a 3-T Ingenia scanner (Philips Healthcare) within a median of 15 days before EAVM (IQR: 3-43 days). A concomitant blood sample was obtained to measure the hematocrit for calculation of ECV. Cine images for evaluation of cardiac morphology and function were acquired in standard cardiac views. LGE images were acquired 10 to 15 minutes after bolus injection of 0.15 mmol/kg of gadoterate meglumine by a whole-heart navigator-gated free-breathing 3D gradient-echo phase sensitive inversion recovery sequence (acquired axial-plane resolution of 1.6×1.6 millimeters). Whole-heart T1 mapping (10 to 12 contiguous slices covering the entire LV with the proximal part of ascending aorta) was performed before and after administration of gadolinium contrast by a modified Look-Locker inversion recovery imaging sequence (reconstructed voxel resolution of $1.25 \times 1.25 \times 10$ millimeters). In patients in whom whole-heart T1 mapping was not possible for logistical reasons, at least 3 short-axis slices (at basal, midventricular, and apical third of the LV) were obtained. Our hardware setup and detailed parameters of the used sequences have been described in detail elsewhere.[12,13]

EAVM. All patients underwent detailed endocardial EAVM of the LV during sinus rhythm (CARTO 3, Biosense Webster) using a 3.5-mm catheter (NaviStar ThermoCool, Biosense Webster) via a transaortic retrograde approach. Intracardiac electrograms were filtered at 30 to 400 Hz (bipolar) and 1 to 240 Hz (unipolar). The fill threshold was set to <15 millimeters.

Limited mapping of the ascending aorta was performed, and the ostium of the left main coronary artery was tagged as an anatomical landmark for image integration. The position within the ostium was confirmed by contrast injection through the irrigation port of the mapping catheter.[14] Radiofrequency energy was delivered only after completing the EAVM.

IMAGE PROCESSING. CMR studies were processed offline using the MASS research software version 2018-EXP (Leiden University Medical Centre, Leiden, the Netherlands). Short-axis ECV maps were calculated pixel-wise, by a standard formula from pre- and postcontrast T1 maps and the patient's blood

TABLE 1   Baseline Characteristics

	All Patients (N = 18)	Without SHD (n = 4)	IHD (n = 6)	NICM (n = 8)
Age, y	57 ± 13	56 ± 13	67 ± 11	51 ± 10
Female	3 (17)	2 (50)	0 (0)	1 (13)
Body surface area, m²	2.1 ± 0.2	2.0 ± 0.2	2.0 ± 0.1	2.2 ± 0.3
Hypertension	9 (50)	2 (50)	4 (67)	3 (38)
Diabetes mellitus	1 (6)	0 (0)	1 (17)	0 (0)
Previous myocardial infarction	6 (33)	0 (0)	6 (100)	0 (0)
Betablockers	14 (78)	2 (50)	6 (100)	6 (75)
ACEI/ARB	10 (56)	1 (25)	5 (83)	4 (50)
Antiarrhythmic drugs	3 (17)	0 (0)	0 (0)	3 (38)
LV ejection fraction, %	48 ± 14	60 ± 3	38 ± 13	48 ± 13
LVEDVI, mL/m²	109 ± 23	93 ± 17	120 ± 19	109 ± 27
LV mass, g	123 ± 25	99 ± 18	138 ± 19	124 ± 24
Presence of any LGE	11 (61)	0 (0)	6 (100)	5 (63)
LGE mass of total LV mass, %	20 (10-29)	0 (0)	27 (22-30)	10 (6-10)

Values are mean ± SD, median (IQR), and n (%), as appropriate.

ACEI/ARB = angiotensin-converting enzyme inhibitor/angiotensin receptor blockers; IHD = ischemic heart disease; LGE = late gadolinium enhancement; LV = left ventricular; LVEDVI = left ventricular end-diastolic volume index; NICM = nonischemic heart disease; SHD = structural heart disease.

hematocrit.[12] Before generating the T1 maps, the image stacks were aligned by an automated registration algorithm.[12]

Isotropic LGE images were reconstructed to 2-mm-thick short-axis slices and analyzed according to our previously described method.[2,14] Presence of LGE was identified by an experienced radiologist and subsequently extracted by an automated thresholding algorithm (using a cut-off of signal intensity (SI) >50% of the maximum SI within the LV myocardium).[14]

Contours of the LV, right ventricle (RV), ascending aorta, and proximal part of the left main coronary artery were delineated by manual segmentation separately for the ECV and LGE image stacks. In each slice, the segmented LV myocardium was divided into 6 equiangular segments starting at the anterior insertion of the RV to the septum. The most apical 1 to 2 slices without a visible LV cavity were excluded. For each LV segment, the mean ECV was calculated by averaging the values of all encompassed voxels; the mean LGE transmurality was calculated from the average transmurality of 17 equidistant centerlines.[4] Contours of the segmented cardiac structures were exported as 3D surface shells (VTK format) compatible with the CARTO system.[2]

IMAGE INTEGRATION AND BACKWARD REGISTRATION OF EAVM DATA ON CMR. Using the CARTO Merge module (Biosense), CMR-derived 3D shells were aligned with EAVM-derived structures using the ostium of the left main coronary artery and all available cavities (LV, RV, aorta) to optimize the alignment.[2,4,14]

The merged EAVM studies were exported as datapoints with a unique ID, containing spatial coordinates, BV, UV, and associated transformation matrix. Using an inversed transformation matrix from the CARTO Merge, the data points were projected back to their corresponding location on the short-axis CMR images. Each of the projected points was coupled with the underlying cardiac segment. The entire merging and inverse registration process was performed separately for ECV and LGE images. Datapoints containing voltage, segment location, and ECV were merged by the unique ID with corresponding datapoints containing segment LGE transmurality. Lastly, to account for the variability of EAVM, all voltage, ECV, and LGE transmurality data were averaged over each cardiac segment. Segments pooled from all patients were submitted for analysis.

STATISTICAL ANALYSIS. Statistical analyses were performed in R software version 3.2 (R Foundation for Statistical Computing). Continuous variables are reported as mean ± SD or median (IQR), according to the normality of the distribution. Between-group comparisons were performed by the Student *t* test, chi square test, or Fisher exact test, as appropriate. A value of $P < 0.05$ was considered statistically significant.

The relationship between voltage and ECV of the pooled cardiac segments was first visually explored on scatterplots with the use of interpolation by local polynomial regression fitting. ECV/voltage relationships in distinct data subsets were evaluated by linear regression and Pearson's correlation. Receiver operating characteristic (ROC) analysis was performed to evaluate the predictive value of decreased endocardial voltage to detect abnormally increased ECV (defined as >95th percentile values obtained in patients without SHD) and to evaluate the predictive value of increased ECV to detect abnormally decreased endocardial voltage (defined as <5th percentile values in patients without SHD).[2,15]

RESULTS

STUDY POPULATION. The study included 18 patients (57 ± 13 years of age, 17% females, LV ejection fraction 48% ± 14%). Of them, 8 had a NICM which had been concluded as idiopathic dilated cardiomyopathy after evaluation according to our standard diagnostic workup, 6 had IHD with a history of prior myocardial infarction, and 4 had no evidence of an SHD or a

primary electrical disease. The patients without SHD served as normal controls.

EAVM was performed as a part of catheter ablation for ventricular tachycardia (n = 11), premature ventricular contractions (n = 5), or as a part of a diagnostic workup in patients with presumed arrhythmic syncope and normal findings on CMR (n = 2). All patients underwent preprocedural 3D LGE-CMR. Of them, 12 (67%) had available whole-heart T1 mapping and 6 (33%) had available T1 mapping in 3 slices. All patients were in sinus rhythm at the time of EAVM and CMR. Baseline characteristics of the patients are provided in **Table 1**.

ELECTROANATOMIC MAPPING AND IMAGE INTEGRATION.
On average, EAVM contained 227 ± 68 mapping points per patient. The mean surface registration error between the EAVM- and CMR-derived LV endocardial shells was 4.5 ± 1.8 millimeters. In total, 628 cardiac segments with merged voltage, ECV, and LGE-transmurality data were available for the analysis (37 ± 15 segments per patient). The average segment voltage was calculated from a mean of 8 ± 5 mapping points per segment.

ECV AND ENDOCARDIAL VOLTAGES.
Table 2 summarizes ECV and endocardial voltage data of the LV myocardium according to the etiology and presence of LGE. In patients without SHD, the mean ECV was 28% ± 3% and the 95th percentile ECV (considered as a cutoff for abnormally increased ECV) was 33%. Regardless of the etiology, ECV was significantly increased in segments with LGE compared to segments without LGE. ECV of segments with LGE did not differ between IHD and NICM, but ECV of segments without LGE was significantly increased in NICM compared to IHD. Moreover, compared to patients without SHD, both IHD and NICM had increased ECV in the entire myocardium and in the segments without LGE (**Table 2**).

The median bipolar and unipolar voltages in patients without SHD were 4.9 mV (IQR: 4.0-6.6 mV) and 14.1 mV (IQR: 9.6-16.8 mV). The 5th percentile voltage values (considered as cutoff for abnormally decreased voltages) were 2.9 mV and 6.7 mV, respectively. BV and UV of the entire LV were significantly reduced in IHD and NICM compared to patients without SHD. If only segments without LGE were analyzed, the average BV remained significantly reduced in IHD and NICM (4.7 mV and 4.6 mV, respectively), whereas UV was significantly reduced only in NICM. Neither the average ECV nor voltages of the entire LV differed between NICM and IHD despite lower LV ejection fraction in the latter group (48% ± 12% vs 38% ± 13%) (**Table 2**).

TABLE 2	ECV and Endocardial Voltage According to the Etiology and the Presence of LGE			
	All Patients	**Without SHD**	**IHD**	**NICM**
All segments, n	628	177	261	190
ECV, %	35 ± 10	28 ± 3	37 ± 11[a]	38 ± 9[a]
Bipolar voltage, mV	4.6 ± 2.5	5.7 ± 2.6	4.0 ± 2.6[a]	4.3 ± 2.0[a]
Unipolar voltage, mV	11.9 ± 5.5	13.8 ± 4.9	11.1 ± 5.6[a]	11.1 ± 5.4[a]
Segments without LGE, n	499	177	171	151
ECV, %	31 ± 6	28 ± 3	32 ± 7[a]	36 ± 6[a,b]
Bipolar voltage, mV	5.0 ± 2.3	5.7 ± 2.6	4.7 ± 2.3[a]	4.6 ± 1.8[a]
Unipolar voltage, mV	13.0 ± 5.2	13.8 ± 4.9	13.2 ± 5.2	11.9 ± 5.4[c,d]
Segments with LGE, n	129	0	90	39
ECV, %	48 ± 11[e]	N/A	46 ± 10[e]	47 ± 14[e]
Bipolar voltage, mV	2.8 ± 2.6[e]	N/A	2.7 ± 2.7[e]	3.2 ± 2.4[e]
Unipolar voltage, mV	7.4 ± 4.1[e]	N/A	7.0 ± 4.0[e]	8.1 ± 4.4[e]

Values are mean ± SD. [a]= significant difference between IHD and without SHD or between CMP and without SHD (P < 0.05 and P < 0.001, respectively). [b]= significant difference between NICM and IHD (P < 0.05 and P < 0.001, respectively). [c]=significant difference between NICM and IHD (P < 0.05). [d]=significant difference between NICM and IHD (P < 0.001). [e]= significant difference between segments with LGE and without LGE within one patient group (P < 0.001 in all cases).

ECV = extracellular volume; N/A = not applicable; other abbreviations as in **Table 1**.

RELATIONSHIP BETWEEN ECV AND ENDOCARDIAL VOLTAGE.
Overall, there was a significant inverse association between endocardial voltage and ECV (**Table 3, Central Illustration**). The association was stronger in abnormal myocardium with increased ECV of >33% or decreased voltage with BV of <2.9 mV or UV of <6.7 mV compared to the myocardium with normal ECV or voltage (**Table 3**). No significant correlation was found between ECV and either BV or UV in segments with ECV of ≤31% and ECV of ≤30%, respectively. The correlation between ECV and voltage was more robust in segments with LGE compared to segments without LGE. Both BV and UV were inversely associated with LGE transmurality (beta = -0.04 and -0.09 in univariate analysis, respectively; P < 0.001 for both).

A similar pattern of the voltage-ECV relationship was also found in a point-by-point analysis which compared voltage of the mapping points with local ECV without calculating the average for cardiac segments, and also in a subanalysis of patients with available whole-heart T1 mapping (Supplemental Tables 1 and 2, Supplemental Figures 1 and 2).

ENDOCARDIAL VOLTAGE MAPPING TO PREDICT ABNORMAL ECV.
Both BV and UV were significant predictors of abnormally increased ECV of >33% with area under the ROC curve (AUC) of 0.71 (95% CI: 0.67-0.75) and 0.75 (95% CI: 0.71-0.79), respectively (**Figure 1**). The sensitivity, specificity, and accuracy to detect abnormal myocardium by decreased voltage was for BV of <0.5 mV: 100%, 55%, and 56%; for BV of <1.5 mV: 96%, 58%, and 61%; for BV of <2.9 mV: 75%, 63%, and 66%; UV of <6.7 mV: 83%, 63%, and

TABLE 3 Correlation Between Voltage and ECV for Selected Subsets

	n	Correlation Coefficient	F	Adjusted R²	P Value
BV vs ECV					
All segments	628	−0.47	175	0.21	<0.001
ECV >33%	290	−0.56	132	0.31	<0.001
ECV ≤33%	338	−0.12	5	0.01	0.03
BV <2.9 mV	154	−0.64	105	0.41	<0.001
BV ≥2.9 mV	474	−0.19	16	0.04	<0.001
LGE absent	482	−0.23	27	0.05	<0.001
LGE present	145	−0.65	101	0.41	<0.001
UV vs ECV					
All segments	628	−0.49	201	0.24	<0.001
ECV >33%	290	−0.53	112	0.28	<0.001
ECV ≤33%	338	−0.11	4	0.01	0.046
UV <6.7 mV	123	−0.47	33	0.21	<0.001
UV 6.7 mV	505	−0.25	33	0.06	<0.001
LGE absent	482	−0.23	27	0.05	<0.001
LGE present	145	−0.61	85	0.37	<0.001

The correlation coefficient was calculated using Pearson's test, F-statistics (1 degree of freedom). R² (adjusted) values were calculated by linear regression. P values were calculated using analysis of variance.

BV = bipolar voltage; UV = unipolar voltage; other abbreviations as in **Tables 1 and 2**.

67%; and UV of <8.3 mV: 71%, 65%, and 67%, respectively.

T1 MAPPING TO PREDICT LOW ENDOCARDIAL VOLTAGES. Increased ECV could predict abnormally decreased voltage (BV of <2.9 mV and UV of <6.7 mV) with an AUC of 0.78 (95% CI: 0.74-0.83) and 0.84 (95% CI: 0.79-0.88), respectively. A cutoff value of ECV >41% predicted abnormally decreased BV with a sensitivity of 51% and a specificity of 93%, and a cutoff value of ECV >36% predicted abnormally decreased UV with a sensitivity of 84% and specificity of 76% (**Figure 1**).

DISCUSSION

This is the first in vivo study in humans to systematically compare CMR-derived ECV values, as a surrogate of fibrosis, with LV endocardial voltage obtained by EAVM, as a surrogate of excitable myocardium. The unique feature of this study is the use of advanced methods that included whole-heart T1 mapping (instead of comparing only 1 septal region of interest) and precise image integration which allowed for direct comparison of EAVM and CMR data of corresponding segments.[9-11]

The main findings can be summarized as follows. 1) Based on control patients without SHD, ECV of >33% was identified as a cutoff for abnormally increased ECV, and BV of <2.9 mV and UV of <6.7 mV were identified as cutoffs for abnormally decreased endocardial voltage. 2) Compared to patients without SHD, patients with NICM and IHD had significantly increased ECV also in segments without LGE. 3) There was a significant inverse relationship between ECV and both BV and UV for ischemic and nonischemic etiologies. The ECV/voltage relationship was more robust in myocardium with abnormally increased ECV (>33%) or abnormally decreased voltage (BV <2.9 mV or UV< 6.7 mV), but it was weak in myocardium with normal ECV and/or endocardial voltage.

DEFINITION OF ABNORMAL MYOCARDIAL VOLTAGE. The use of binary voltage cutoffs to discern abnormal myocardium by EAVM is widely implemented in clinical practice, although the evidence supporting their use is limited.[16] Currently, the most frequently used cutoffs for abnormal voltage are BV of <1.5 mV and UV of <8.3 mV. These cutoffs were derived from the 5th percentile voltage values obtained by EAVM in 4 and 6 healthy persons with the average age of 37 ± 12 years and 36 ± 18 years, respectively.[1,15]

Using the same approach in our patients without SHD, we found a higher cutoff for abnormal BV (<2.9 mV) but a lower cutoff for abnormal UV (<6.7 mV). It is possible that these differences may be due to aging and related fibrosis and/or loss of viable myocardium in our relatively older population (mean age, 57 ± 13 years). A global reduction of the viable myocardial mass may be more sensitively detected by UV compared to BV because of a larger field of view of the UV mapping. On the other hand, the voltage cutoffs found in this study corroborate our previously reported cutoffs of BV ≥3.0 mV and UV ≥6.7 mV for nondiseased myocardium, which were derived in a similar fashion from the myocardium remote from infarct scar detected by LGE-CMR in IHD patients without LV remodeling.[2]

A cutoff of BV<1.5 mV to detect compact transmural scar has been validated in an animal infarct model.[17] BV mapping to detect intramural or subepicardial nonischemic scar or infarct gray zones is less accurate, which has been attributed to the limited field of view of BV mapping.[4,14] UV has been suggested to better delineate nonischemic scars, and various cutoff values for its use have been validated against LGE-CMR. However, dependent on the LGE-CMR acquisition and postprocessing method different cu-off values to detect nonischemic scar, ranging from 5.64 mV (SI>SI$_{mean}$ remote myocardium + 6 SD) to 8.01 mV (SI >30% of SI$_{max}$) have been reported.[6,14,18,19]

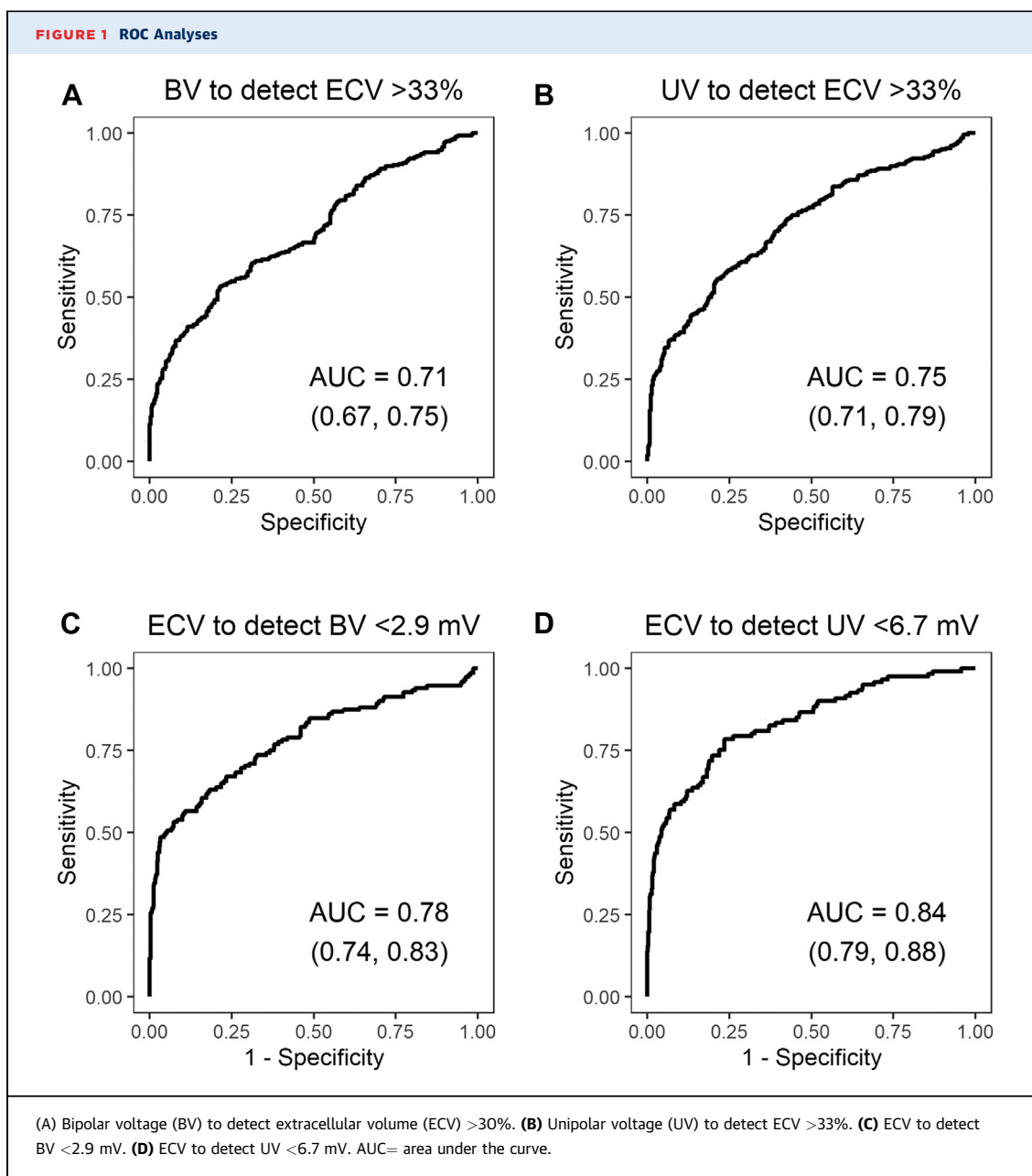**CENTRAL ILLUSTRATION** Workflow and Main Results
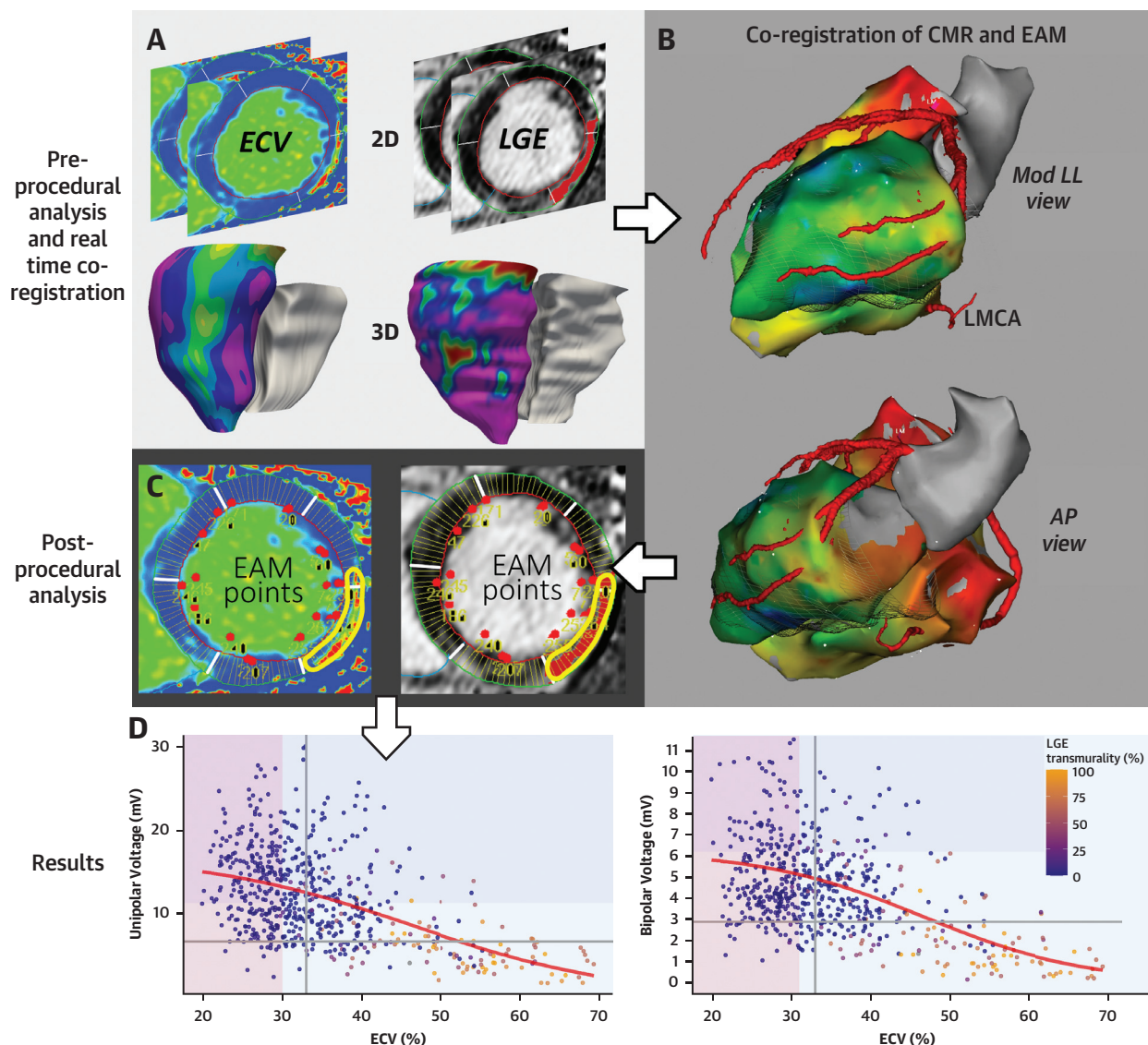
Sramko M, et al. J Am Coll Cardiol EP. 2023;9(6):740–748.

(A) Image processing of cardiac magnetic resonance (CMR) imaging data and conversion from 2-dimensional (2D) data to a 3-dimensional (3D) shell. **(B)** Coregistration of processed CMR and electroanatomical voltage mapping (EAVM) data. **(C)** Reverse projection of EAVM data on the original CMR data using the reversed registration matrix. **(D)** The scatter plots show the relationship between bipolar voltage (BV) and extracellular volume (ECV) **(right panel)** and UV and ECV **(left panel)** in segments pooled from all patients. Each datapoint represents the average voltage and ECV of a cardiac segment. The **gray lines** represent the cutoffs for abnormally increased ECV (>33%) and decreased voltage (BV of <2.9 mV and unipolar voltage [UV] of <6.7 mV) derived from the patients without structural heart disease. The **color-shaded areas** depict data subsets where the voltage/ECV was weak. **Color-coded regions** show the average late gadolinium enhancement (LGE) transmurality of a corresponding segment on LGE sequences. LGE starts to appear mostly in segments with ECV >45%. AP = anterior posterior; EAM = electroanatomical mapping; Mod LL = modified left lateral.

RELATIONSHIP BETWEEN ENDOCARDIAL VOLTAGE AND ECV. ECV assessed by T1 mapping can better evaluate diffuse fibrosis than LGE-CMR.[7] Diffuse myocardial fibrosis can be found in NICM patients and also in noninfarcted myocardium in IHD patients with remodeled LV.[2] In fact, in this study we found abnormally increased ECV which was accompanied by decreased voltage in patients with NICM and IHD even in the myocardium without apparent LGE.

FIGURE 1 ROC Analyses

(A) Bipolar voltage (BV) to detect extracellular volume (ECV) >30%. **(B)** Unipolar voltage (UV) to detect ECV >33%. **(C)** ECV to detect BV <2.9 mV. **(D)** ECV to detect UV <6.7 mV. AUC= area under the curve.

Another important observation was a sigmoid shape of the ECV/voltage relationship curve: whereas there was a significant inverse linear ECV/voltage relationship in myocardium with intermediate fibrosis (ECV between 30% and 60%), the relationship curve flattened (ie, the correlation weakened) in densely fibrotic tissue (ECV >60%) and also in healthy tissue with minimal fibrosis (ECV <30%-31%). This finding corroborates a previous study from our group that found a similar relationship between endocardial voltage with fibrosis assessed by whole-heart

histology.[3] The observed ECV/voltage relationship highlights the fact that an oversimplified use of arbitrary binary or ternary voltage cutoffs to delineate fibrosis may limit the diagnostic accuracy of EAVM in different patient populations.

At last, compared to only postcontrast T1 mapping, which is reported in milliseconds and is dependent on CMR field, sequence type, and timing after gadolinium administration, the assessment of ECV takes into consideration native T1 values and blood hematocrit and is more reproducible across different CMR

scanner vendors.[20] As such, the established thresholds of ECV in this study can be further validated by future studies and implemented across centers.

CLINICAL IMPLICATIONS. CMR-derived 3D-shells with color-coded ECV values projected on the surface could be registered with EAVM during catheter ablation for ventricular arrhythmia. This information could help localize diseased myocardium, thereby focusing mapping to fibrotic areas. In addition, integration of ECV and EAVM data could help clarify specific characteristics of fibrosis related to sustained ventricular tachycardia in patients with nonischemic substrate. Whether it would also improve detection of the arrhythmic substrate and procedural outcome must be determined by future studies.

STUDY LIMITATIONS. This was a small retrospective study. The sample size was limited by the fact that patients undergoing ablation for ventricular arrhythmias, who do not have implanted cardioverter-defibrillators and are able to undergo preprocedural CMR are relatively rare in clinical practice. This might have led to a selection bias, which was documented by the relatively higher average LV ejection fraction. On the other hand, this enabled us to study patients with a broad range of LV structural remodeling. The sample size was sufficient to confirm significant associations between ECV and voltage and to show the differences in ECV and voltage among different etiologies.

We evaluated the LV voltage by point-by-point contact mapping, as this approach enables a better real-time control of the signal quality. On the other hand, compared to mapping with contemporary multielectrode-electrode catheters, the point-by-point mapping could have led to relative under sampling and uneven distribution of the mapping points. To address this potential bias, we have analyzed average segment data. Moreover, this approach enabled us to study volumes of the same size and compensated the possible registration errors and variability in imaging and image processing.

At last, our proposed voltage cutoffs derived from the "normal" voltage of individuals without SHD have been evaluated to detect abnormal tissue with increased ECV but not detect arrhythmic substrate itself. Whether use of these cutoffs would be superior to the currently used cutoffs must be determined by future studies.

CONCLUSIONS

This study found that contrast-enhanced T1 mapping is reliable in detecting endocardial low voltage area. These findings may help during catheter ablation to identify areas of fibrosis potentially related to ventricular arrhythmias.

ADDRESS FOR CORRESPONDENCE: Dr Katja Zeppenfeld, Willem Einthoven Center for Cardiac Arrhythmia Research and Management, Leiden University Medical Center, Department of Cardiology, P.O. Box 9600, 2300 RC Leiden, the Netherlands. E-mail: k.zeppenfeld@lumc.nl.

PERSPECTIVES

COMPETENCY IN PATIENT CARE AND PROCEDURAL SKILLS: The use of preprocedural imaging to identify fibrosis and potential arrhythmic substrate has been proven in clinical practice. Assessment of ECV by postcontrast T1 mapping can be valuable in patients with diffuse fibrosis not detectable by LGE. Real-time integration of ECV to EAVM could help focusing catheter mapping to the diseased myocardium, thereby decreasing procedural time. In addition, the knowledge of the presence of increased fibrosis could improve identification of areas with diffuse fibrosis harboring the arrhythmic substrate.

TRANSLATIONAL OUTLOOK: Although the technique has improved over the previous decade, assessment of ECV by postcontrast T1 mapping is still time-consuming. We hypothesize that, with the introduction of automated image processing using artificial intelligence, in the future it will be feasible to implement real-time ECV data to EAVM.

REFERENCES

1. Marchlinski FE, Callans DJ, Gottlieb CD, Zado E. Linear ablation lesions for control of unmappable ventricular tachycardia in patients with ischemic and nonischemic cardiomyopathy. *Circulation.* 2000;101:1288–1296.

2. Sramko M, Abdel-Kafi S, van der Geest RJ, et al. New adjusted cutoffs for "normal" endocardial voltages in patients with post-infarct LV remodeling. *J Am Coll Cardiol EP.* 2019;5:1115–1126.

3. Glashan CA, Androulakis AFA, Tao Q, et al. Whole human heart histology to validate electro-anatomical voltage mapping in patients with non-ischaemic cardiomyopathy and ventricular tachycardia. *Eur Heart J.* 2018;39:2867–2875.

4. Wijnmaalen AP, van der Geest RJ, van Huls van Taxis CF, et al. Head-to-head comparison of contrast-enhanced magnetic resonance imaging and electroanatomical voltage mapping to assess post-infarct scar characteristics in patients with ventricular tachycardias: real-time image integration and reversed registration. *Eur Heart J*. 2011;32: 104–114.

5. Piers SR, Leong DP, van Huls van Taxis CF, et al. Outcome of ventricular tachycardia ablation in patients with nonischemic cardiomyopathy: the impact of noninducibility. *Circ Arrhythm Electrophysiol*. 2013;6:513–521.

6. Desjardins B, Yokokawa M, Good E, et al. Characteristics of intramural scar in patients with nonischemic cardiomyopathy and relation to intramural ventricular arrhythmias. *Circ Arrhythm Electrophysiol*. 2013;6:891–897.

7. Miller CA, Naish JH, Bishop P, et al. Comprehensive validation of cardiovascular magnetic resonance techniques for the assessment of myocardial extracellular volume. *Circ Cardiovasc Imaging*. 2013;6:373–383.

8. Nakamori S, Dohi K, Ishida M, et al. Native T1 mapping and extracellular volume mapping for the assessment of diffuse myocardial fibrosis in dilated cardiomyopathy. *J Am Coll Cardiol Img*. 2018;11:48–59.

9. Chen Z, Sohal M, Voigt T, et al. Myocardial tissue characterization by cardiac magnetic resonance imaging using T1 mapping predicts ventricular arrhythmia in ischemic and non-ischemic cardiomyopathy patients with implantable cardioverter-defibrillators. *Heart Rhythm*. 2015;12:792–801.

10. Puntmann VO, Carr-White G, Jabbour A, et al. T1-mapping and outcome in nonischemic cardiomyopathy: all-cause mortality and heart failure. *J Am Coll Cardiol Img*. 2016;9:40–50.

11. Muser D, Nucifora G, Castro SA, et al. Myocardial substrate characterization by CMR T1 mapping in patients with NICM and no LGE undergoing catheter ablation of VT. *J Am Coll Cardiol EP*. 2021;7(7):831–840.

12. Tao Q, van der Tol P, Berendsen FF, Paiman EHM, Lamb HJ, van der Geest RJ. Robust motion correction for myocardial T(1) and extracellular volume mapping by principle component analysis-based groupwise image registration. *Journal of magnetic resonance imaging. J Magn Reson Imaging*. 2018;47(5):1397–1405.

13. Bizino MB, Tao Q, Amersfoort J, et al. High spatial resolution free-breathing 3D late gadolinium enhancement cardiac magnetic resonance imaging in ischaemic and non-ischaemic cardiomyopathy: quantitative assessment of scar mass and image quality. *Eur Radiol*. 2018;28:4027–4035.

14. Piers SR, Tao Q, de Riva Silva M, et al. CMR-based identification of critical isthmus sites of ischemic and nonischemic ventricular tachycardia. *J Am Coll Cardiol Img*. 2014;7:774–784.

15. Hutchinson MD, Gerstenfeld EP, Desjardins B, et al. Endocardial unipolar voltage mapping to detect epicardial ventricular tachycardia substrate in patients with nonischemic left ventricular cardiomyopathy. *Circ Arrhythm Electrophysiol*. 2011;4:49–55.

16. Sramko M, Hoogendoorn JC, Glashan CA, Zeppenfeld K. Advancement in cardiac imaging for treatment of ventricular arrhythmias in structural heart disease. *Europace*. 2019;21:383–403.

17. Reddy VY, Wrobleski D, Houghtaling C, Josephson ME, Ruskin JN. Combined epicardial and endocardial electroanatomic mapping in a porcine model of healed myocardial infarction. *Circulation*. 2003;107:3236–3242.

18. Piers SR, Tao Q, van Huls van Taxis CF, Schalij MJ, van der Geest RJ, Zeppenfeld K. Contrast-enhanced MRI-derived scar patterns and associated ventricular tachycardias in nonischemic cardiomyopathy: implications for the ablation strategy. *Circ Arrhythm Electrophysiol*. 2013;6: 875–883.

19. Sasaki T, Miller CF, Hansford R, et al. Impact of nonischemic scar features on local ventricular electrograms and scar-related ventricular tachycardia circuits in patients with nonischemic cardiomyopathy. *Circ Arrhythm Electrophysiol*. 2013;6:1139–1147.

20. Haaf P, Garg P, Messroghli DR, Broadbent DA, Greenwood JP, Plein S. Cardiac T1 mapping and extracellular volume (ECV) in clinical practice: a comprehensive review. *J Cardiovasc Magn Reson*. 2016;18:89.

KEY WORDS extracellular volume, T1 mapping, fibrosis, voltage, image integration

---

APPENDIX For supplemental tables and figures, please see the online version of this paper.